THE JOURNAL OF PHYSICAL CHEMISTRY C
A JOURNAL OF THE AMERICAN CHEMICAL SOCIETY

pubs.acs.org/JPCC

Article

Dynamics of Water Dissociative Adsorption on TiO_2 Anatase (101) at Monolayer Coverage and Below

Francesca Fasulo, GiovanniMaria Piccini, Ana B. Muñoz-García, Michele Pavone,* and Michele Parrinello*

Cite This: *J. Phys. Chem. C* 2022, 126, 15752−15758

Read Online

ACCESS | Metrics & More | Article Recommendations

ABSTRACT: TiO_2 anatase is a functional material that is exploited in several technological devices from photovoltaics to energy storage, water splitting, and solar-to-fuel photocatalysis. In this context, numerous theoretical studies addressed the interaction of water with the most stable anatase (101) surface and reported undissociated molecular adsorption. However, recent experiments on such surface facet at low water coverage pointed out the presence of OH groups. Motivated by these findings, we report here a first-principles investigation on the adsorption and dissociation at low (θ = 0.25) and full (θ = 1) coverage of the first water monolayer at the (101) anatase surface at 300 K with metadynamics. Our simulations show barrierless water adsorption, and at the same time, the dynamic nature of titania−water interactions allows for the dissociation of water and the possible formation of a partial hydroxylated surface at room temperature. These results highlight the relevance of dynamic in modeling surface−water interactions and provide new insights into the physicochemical properties of the pristine anatase TiO_2(101) surface in an aqueous environment.

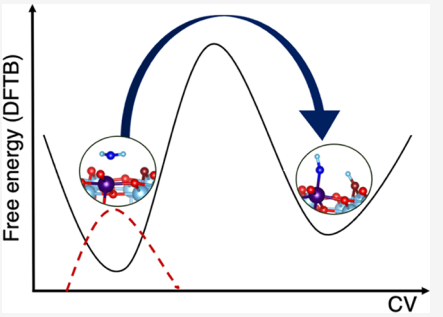

INTRODUCTION

Artificial photosynthesis aims at the efficient conversion and storage of solar energy to fuels or high-energy chemicals.[1,2] Water splitting into oxygen and molecular hydrogen and reduction of carbon dioxide to methanol or other products are both reverse combustion processes that can be enhanced by combining sunlight and photoelectrocatalysis.[3−6] To this end, several semiconductors have been investigated as potential photocatalysts (CdS, ZrO_2, Ga_2O_3, and Cu_2O are few examples).[7−11] Among them, titania (TiO_2) has emerged as a sustainable photoelectrode thanks to its low cost, stability, and nontoxicity.[12−14] Moreover, nanostructured titania has proven to be very effective in a large variety of photocatalytic applications in aqueous solutions from water splitting to photodegradation of organic pollutants.[15−21] In this framework, elucidating the structure and reactivity of titania−water interfaces is thus crucial for improving the efficiency and selectivity of solar-to-fuel processes, especially in an aqueous environment. Among TiO_2 polymorphs, anatase is the most relevant because it is the most stable at the nanoscale, and its (101) surface termination is the most exposed in nanoparticles.[13,22−24] Several experimental and theoretical studies have addressed the reactivity of water on this facet,[25−39] but there are still open questions such as the roles of undercoordinated fivefold Ti surface species (Ti_{5C}) and water coverage (θ = no. H_2O adsorbed/no. Ti_{5C} on the surface first layer) on the subtle equilibrium between molecular and dissociative adsorption of water molecules.[27,34,37−39]

The first water layer (θ = 1) is defined by the H_2O molecules adsorbed onto all Ti_{5C} sites. The second layer consists of water molecules that interact via H-bonding to the TiO_2 surface oxygen atoms (at the twofold O_{2C} sites): these H···O_{2C} H-bonds have an average length of ∼1.9 Å. The third layer is given by water−water interactions and the molecules farther than this from the surface are regarded as bulk water.[26,31,34] In particular, ab initio molecular dynamics (AIMD), based on density functional theory (DFT), has been applied to address the reactivity of water at different coverage[26−31] by performing simulations at 160 K, which is the lowest temperature peak in the temperature-programmed desorption (TPD) spectra.[36] AIMD results show that at low θ, molecular adsorption is largely favored, with an adsorption energy of about 0.8 eV, while water can easily dissociate on an oxygen-deficient surface, due to an increase of O_{2C} basicity.[26] In molecular adsorption, H_2O presents a dative bond with an undercoordinated Ti_{5C} site at about 2.3 Å, while in dissociative

Received: May 4, 2022
Revised: August 1, 2022
Published: August 13, 2022

adsorption, a OH group binds covalently to Ti_{5C} at about 1.8 Å, and H binds to O_{2C} sites; thus, there is formation of two surface hydroxyl groups, a terminal hydroxyl on Ti_{5C} and a bridging hydroxyl, corresponding to protonated O_{2C} (see Scheme 1).[25]

Scheme 1. Schematic Representations of (a) Molecular (H_2O in Red) and (b) Dissociative (OH in Blue) Configurations at the Anatase TiO_2(101) Surface

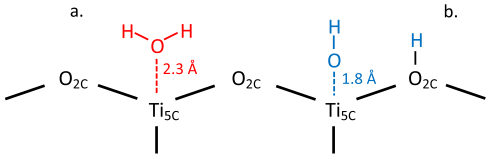

Oxygen vacancies can strongly affect the structures of water mono- and bilayer. A water molecule incorporated into the mono- or bilayer on a defective surface can dissociate spontaneously. However, with surface X-ray diffraction (SXRD) data, Nadeem and co-workers[38] observed that an ultrathin water film on the (101) anatase surface at room temperature exhibits a mixture of molecular H_2O (25%) and OH (75%) bound to Ti_{5C} at the contact layer. They also highlighted that water dissociation is delimited to the first water layer. Exposing the TiO_2(101) surface to bulk water, there is only an ordered second monolayer that is molecularly adsorbed above the first one. Further evidence of mixed molecular and dissociative adsorption at room temperature at a higher pressure of water (0.6−6.0 mbar) has also been obtained by photoemission spectroscopy (X-ray photoelectron spectroscopy (XPS)), while water was not dissociated in ultrahigh vacuum (UHV).[39] High-resolution XPS has predicted the presence of OH groups at the stoichiometric TiO_2(101) surface.[40] These results have challenged the accepted model of the water−stoichiometric anatase interface due to controversy about the nature of the first water monolayer on the pristine (101) anatase surface and, especially, whether there is molecular or dissociative adsorption.

In this context, previous DFT-based calculations at low coverage only predicted the molecular adsorption to be the relevant one on stoichiometric anatase surfaces,[25−27] and recent studies based on a hybrid density functional (taking the zero-point energy correction into account)[41,42] and reactive force field molecular dynamics[43] provided evidence of dissociative adsorption, in agreement with experiments.[38−40] However, the experimental temperature dependence suggests that the percentage of dissociated water molecules increases with temperature (25% of molecules dissociate at 220 K and 75% of them at 300 K).[40] Giustino et al.[41] and other recent works[42] investigated only two interface structures: one with only water molecules, and another where 25% of the molecules underwent dissociation. Also, results from molecular dynamics simulations pointed out the variation of terminal OH coverage over TiO_2(101) with temperature, but never reaching 50%.[43] Within this framework, complete and statistically sound characterization of water dynamics at room temperature could provide further insights into molecular versus dissociative adsorption, exploring all of the possible hydroxylated TiO_2(101) surfaces (25, 50, 75, and 100%) in closer resemblance to the experiment.

Therefore, here, we report metadynamics[44] MD simulations of water adsorption and dissociation on the anatase TiO_2(101) surface, at low (θ = 0.25) and full (θ = 1) coverage at 300 K. We employed the self-consistent charge density functional tight binding (SCC−DFTB) level of theory in our simulations.[45,46] Such an approach provides reliable results on structures, electronic features, and energetics for the water−titania interface, in qualitative agreement with DFT ones but at a much-reduced computational cost.[34,47]

The metadynamics approach allows an enhanced sampling of reactive events by introducing an additional bias potential along the system trajectory, acting on a selected number of degrees of freedom (named collective variables, CVs). Thus, the system is discouraged from remaining in minimum-energy configurations that have been already sampled, allowing the free energy surface (FES) as a function of the chosen CVs[44] to be reconstructed. This approach also works very well for systems that present high free energy barriers, as in the case of water dissociation at the anatase TiO_2(101) stochiometric surface.[25−27,34]

METHODS AND COMPUTATIONAL DETAILS

The CP2K/Quickstep package[48] was used to perform static geometry optimizations and for metadynamics simulations, combined with the PLUMED package.[49]

Canonical sampling through a velocity rescaling (CSVR) thermostat[50] with a target temperature of 300 K and a time constant of 0.05 ps was used to impose NVT conditions to the system, while a time step of 0.5 fs was used to ensure reversibility. The pre-equilibration simulation was run for 15 ps, and then the systems were allowed to evolve for other 12 ns to ensure convergence of FES.

For these simulations, the Gaussian hills sigma was 0.1 and 0.3 Å for dissociation at θ = 0.25, θ = 1 and adsorption processes, respectively. The height was 4.0 kJ/mol, while the bias factor was 50, and the deposition rate was 100 steps.

The convergence of the electronic structure and the forces were relaxed to less than 10^{-6} au with the k-sampling restricted to the Γ-point.

The (101) anatase surface is modeled with a three-bilayer slab, all relaxed during the geometry optimization. We have employed a surface slab approach[51] with a vacuum of 20 Å in the direction perpendicular to the surface to avoid interactions between images; 1 × 2 supercells with 24 TiO_2 formula units were employed (a = 10.47 Å, b = 7.59 Å). Such a model is extensively proven to be adequate to describe anatase surface properties.[13,23,25−27,31,34,35,52]

For the DFT study, the generalized gradient approximation (GGA) within its PBE formulation[53] was used to account for exchange-correlation effects. The 3s, 3p, 3d, and 4s electrons of Ti atoms and the 2s and 2p electrons of O atoms were considered valence electrons, and Goedecker−Teter−Hutter (GTH) pseudopotentials were used to treat the core electrons. Single-point energy calculations are carried out on selected geometries with the HSE06 hybrid functional. Double-ζ basis functions with one set of polarization functions (double-ζ valence polarized (DZVP)) were used as basis sets with a plane wave cutoff of 380 Ry.

RESULTS AND DISCUSSION

For performing our metadynamics MD simulations, we selected the MATSCI parameterization of DFTB, which is

https://doi.org/10.1021/acs.jpcc.2c03077
J. Phys. Chem. C 2022, 126, 15752−15758

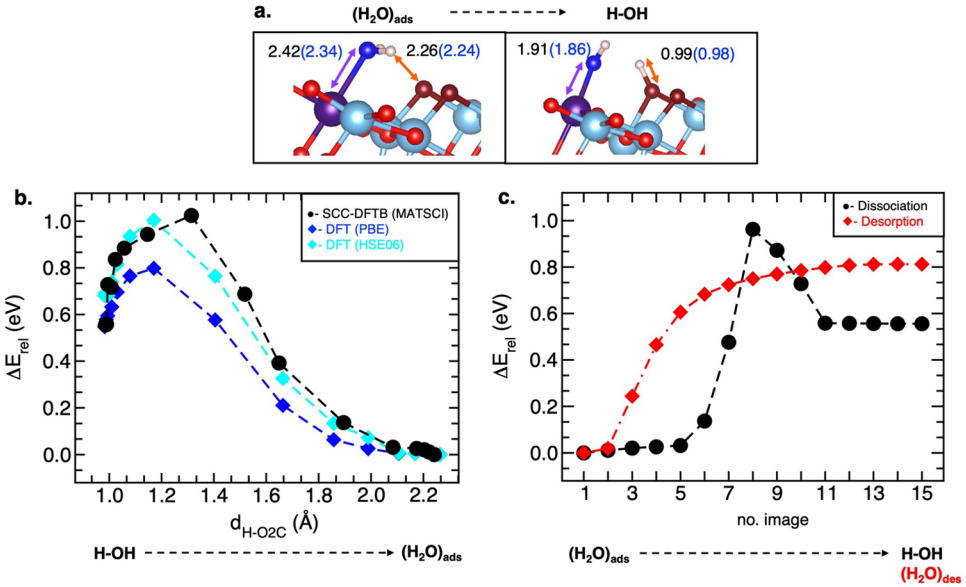

Figure 1. (a) Molecular and dissociative adsorbed states. Color legend: O (red), Ti (light blue), O_{2C} (dark red), Ti_{5C} (violet), water oxygen O_W (blu), H (white). Equilibrium distances (in Å) are reported for SCC−DFTB(MATSCI) (black font) and DFT(PBE) (blue font). (b) Dissociative reaction path computed with SCC−DFTB(MATSCI) (black circles), DFT(PBE) (blue diamonds), and DFT(HSE06) (cyan diamonds). (c) SCC−DFTB(MATSCI) results for desorption (red diamonds) and dissociation (black circles) reactions.

extensively employed in materials science and has been also tested specifically for the water−titania interface.[34,47,54] Since the subtle balance between water−water and water−surface interactions is key to molecular versus dissociative adsorption, we tested the DFTB(MATSCI) level of theory against DFT(PBE) and DFT(HSE06) by computing the dissociation reaction path for a single water molecule at the TiO_2(101) surface with the NEB approach,[55] as implemented in CP2K (see Figure 1).[48]

The NEB procedure was carried out employing 15 intermediate images. To follow the dissociation path (from molecular $(H_2O)_{ads}$ to dissociated (H−OH) adsorbed water), we reported on the *x*-axis the values of distances between surface oxygen O_{2C} and the hydrogen water atom d_{H-O2C} (see the orange arrow in Figure 1a). ΔE_{rel} is the relative energy with respect to the lowest energy state, i.e., $(H_2O)_{ads}$.

The computed structural parameters for minimum-energy configurations are similar between the DFTB and DFT levels of theory and both methods predict the molecular adsorption to be more favorable than the dissociated one. We found that the ΔE_{rel} between molecular adsorption and dissociation is slightly higher at the DFT(HSE06) level of theory (∼0.6 eV) than those at DFT(PBE) and DFTB(MATSCI) (∼0.5 eV). The activation energy for water dissociation by the DFTB-(MATSCI) level of theory is higher (∼0.2 eV) than that by DFT(PBE) but matches the most reliable DFT(HSE06) reaction barrier. Overall, the comparison between DFTB, GGA, and hybrid functional shows that DFTB(MATSCI) provides a rather accurate electronic description of the water−titania interfaces at an extremely reduced computational cost,[56,57] and we can consider DFTB(MATSCI) to be reliable and effective for our investigations.

Figure 1 also shows the comparison between adsorption and dissociation paths computed by NEB with DFTB(MATSCI): the activation energies for the two processes differ by ∼0.2 eV, thus implying that the two processes occur at different time scales, thus allowing us to perform two independent metadynamics simulations, one for adsorption and another for dissociation because the two processes are not directly competing.

For simulations of water adsorption, we choose CVs as the number of adsorbed but not dissociated water molecules onto the titania surface. Considering our TiO_2(101) 1 × 2 slab model with 4 Ti_{5C} surface sites, the CV changes from 0 for no adsorbed molecules to 4 for the fully molecular adsorbed first water monolayer: the CV number depends on the distances between surface Ti_{5C} and the water oxygen atom O_W that are less than 3 Å (Figure 2). For water dissociation at 0.25 and 1 coverages, we choose generalized coordination numbers as CVs, employing a rational switching function implemented in

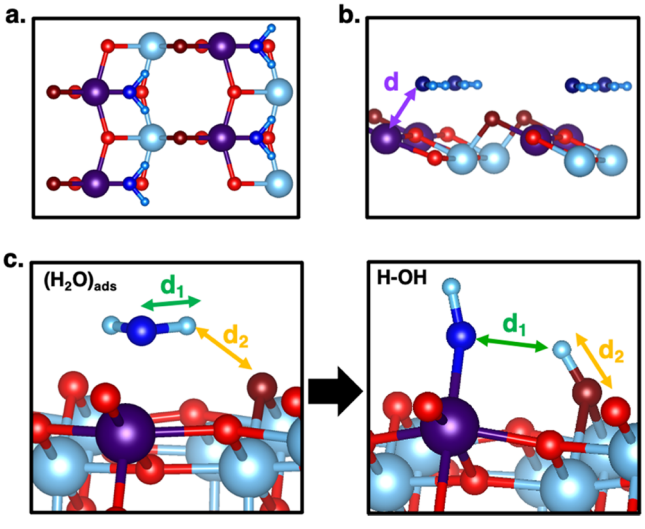

Figure 2. (a) Full coverage (θ = 1) view along the *c*-axis. (b) Distance between Ti_{5C} and O_W (*d*, violet arrow). (c) Distances between H with O_W (d_1, green arrow) and O_{2C} (d_2, orange arrow). Color legend: O (red), Ti (light blue), O_{2C} (dark red), Ti_{5C} (violet), O_W (blue), and H (white).

https://doi.org/10.1021/acs.jpcc.2c03077
J. Phys. Chem. C 2022, 126, 15752−15758

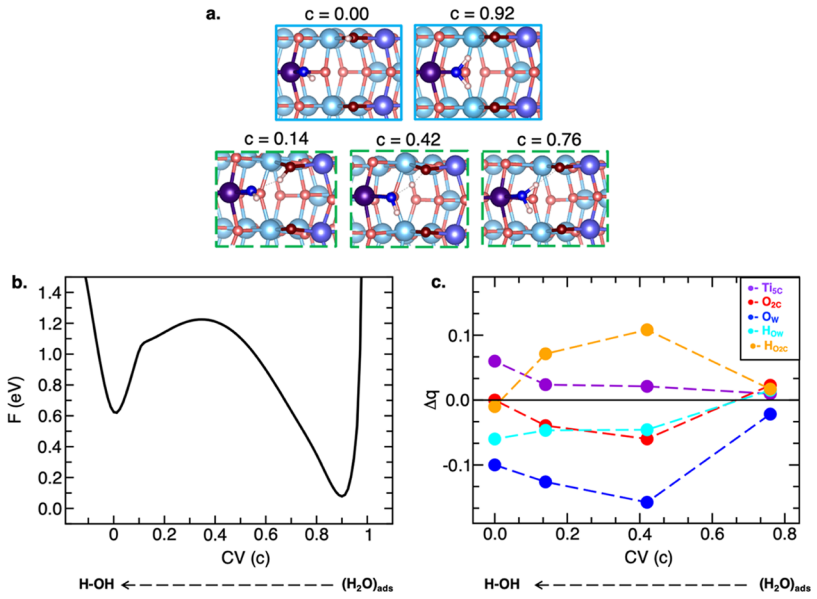

Figure 3. (a) Selected images with values of CVs c from metadynamics dissociation trajectory at $\theta = 0.25$ (top view, color legend as in Figure 1). (b) FES for the dissociation process at $\theta = 0.25$. (c) Mulliken population analysis of atomic effective charges (q, at the DFT-PBE level of theory) on Ti_{5C} (violet), O_{2C} (red), O_W (blue), H atom bond to O_W (light blue), and H atom bond to O_{2C} (orange). $\Delta q = [q \text{ at c}] - [q \text{ at } c = 0.92\ (H_2O)_{ads}]$.

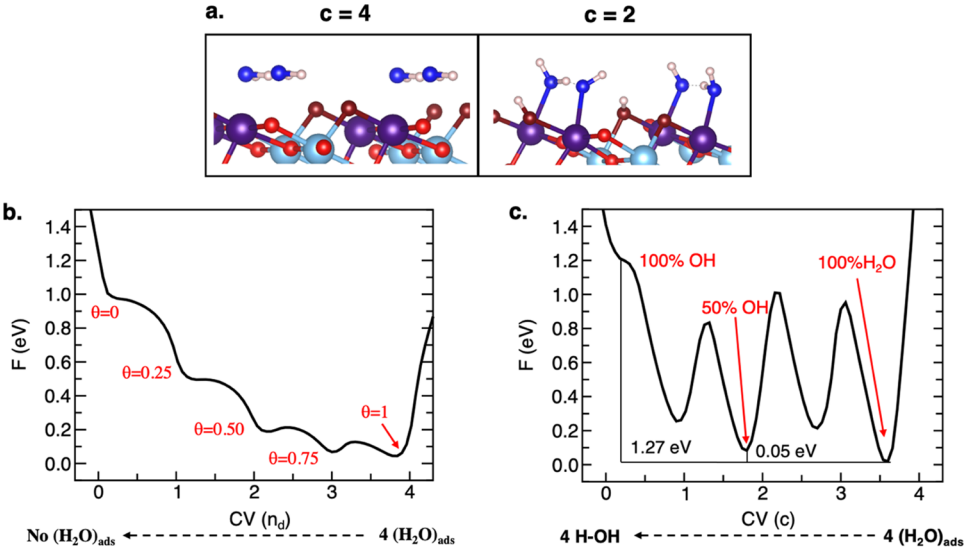

Figure 4. (a) Selected images for CVs $c = 4$ (4 $(H_2O)_{ads}$) and 2 (mix state)). (b) FES for the molecular adsorption process at coverage $\theta = 1$. (c) FES for the dissociation process at coverage $\theta = 1$.

PLUMED.[49] These CVs, named, n_{d1} and n_{d2}, account for the number of O−H distances that are less than the target value: d_1 is the distance between water oxygen (O_W) and hydrogen atoms, while d_2 is the distance between surface oxygen O_{2C} and hydrogen water atoms (Figure 2). The target values for the two chosen CVs, d_1 and d_1, are both selected at 1.3 Å, while the n parameter of the switching function is 8.

We are conscious that the interconversion process takes place via adsorption and desorption. However, since the CV is such that allows reversible transition between the states, we can trust the results on the difference in FES between states, while a proper evaluation of the transition barrier would require a different and more complex CV accounting for both adsorption and dissociation processes.

Therefore, when a H_2O molecule is adsorbed but undissociated, n_{d1} and n_{d2} are 2 and 0, respectively, while for the dissociated state, both are 1.

Given the simplicity of this description, these two variables could be easily combined into a simpler one-dimensional linear combination ($c = 0.5\ n_{d1} - 0.5\ n_{d2}$), that is, 1 for molecular adsorption and 0 for dissociative. Considering the full coverage with a molecule for each Ti_{5C} ($\theta = 1$), we employed the same CV c given by the combination of n_{d1} and n_{d2}: c goes from 0 (all dissociated) to 4 (no dissociated water).

From the analysis of the metadynamics simulations at low coverage ($\theta = 0.25$), we found the undissociated adsorbed water to be the lowest energy state as found in NEB calculations. The resulting $\Delta E_{diss-ads}$ is 0.54 eV and the FES (Figure 3) presents an energy barrier of 1.14 eV to water dissociation. These results agree with the previous DFT

https://doi.org/10.1021/acs.jpcc.2c03077
J. Phys. Chem. C 2022, 126, 15752−15758

calculations and generally support the dominant molecular adsorption at the dilute limit on the stoichiometric TiO_2(101) surface.[25,26,58,59]

Furthermore, we performed an analysis of effective atomic charges (Mulliken population analysis) at the DFT(PBE) level on selected images along these trajectories and we found the dissociation of water to be heterolytic, with an increase of positive and negative charges on the hydrogen atom that goes onto the anatase surface (H_{Surf}) and on O_W, respectively. This behavior is consistent with water dissociation on other similar metal oxides.[60−63]

These results also validate our method based on the metadynamics at the DFTB(MATSCI) level of theory and the choice of our CVs.

Considering the adsorption of the first water layer (Figure 4a), the calculated adsorption energy per molecule at the DFTB(MATSCI) level of theory (0.67 eV) is closer to Tilocca and Selloni energy (0.69 eV),[25,26] even though the DFTB-(MATSCI) ground state at c = 4 is not rotated as predicted by the DFT level of theory.

By metadynamics simulations of the adsorption process toward the full coverage, we found decreasing activation free energies for the second, third, and fourth water molecules (Figure 4b).

In this case, CVs, named n_d, account for the number of O_W−Ti_{5C} distances (Figure 1a) that are less than 2.8 Å, while the n parameter of the switching function is 8.

The molecular adsorption is easily favored until the formation of the first water monolayer (θ = 1), and the total adsorption free energy is consistent with previous studies at about 0.9 eV.[27] In this first water monolayer, water is preferentially adsorbed as molecules on the Ti_{5C} sites of the anatase (101) surface at room temperature. By comparing Figures 3b and 4c, we also found that water dissociation is more likely to occur at full coverage θ = 1 than at low coverage θ = 0.25.

Figure 4c displays the FES for water dissociation at full coverage; the lowest energy state corresponds to $c \approx 4$, i.e., four adsorbed water molecules and no dissociated ones. This is followed by the $c \approx 2$ state, i.e., two adsorbed water molecules and two dissociated ones (50% dissociative adsorption): this partial hydroxylated state differs by only 0.05 eV (~1 kcal/mol) with respect to the $c \approx 4$ state. Otherwise, the states corresponding to $c \approx 3$ (25% dissociated molecule) and $c \approx 1$ (75% dissociated molecule) are both 0.20 eV higher than the most favorite state (c = 4). The less favorite state is then the full dissociated state (c = 0) that lies at 1.27 eV. Both the states at 0.20 and 1.27 eV above the ground-state configurations are very unlikely to occur.

As previously highlighted by Patrick and Giustino for a hydroxylated surface,[41] we found that the mixed state ($c \approx 2$) can be stabilized by the H-bond interactions between the water molecule and the hydroxylate group (H_2O−OH, Figure 4a). Thus, a partial hydroxylated anatase surface is likely to be observed when water adsorption is at full coverage θ = 1, while a full hydroxylated surface is mostly unfavorable.

Considering the structural features of water dynamics, we found that the formation of the first molecularly adsorbed water layer does not induce any significant variations of average Ti_{5C}−O_{2C} bond distance ($d_{Ti5C-O2C}$), while at increasing water dissociation, $d_{Ti5C-O2C}$ increases from 1.87 ± 0.02 Å (at CV $c \approx 4$) to 2.18 ± 0.05 Å (at CV $c \approx 0$). This large expansion of the Ti_{5C}−O_{2C} bond length is due to the protonation of O_{2C} in the fully dissociated aqueous interface. When only half of the adsorbed water molecules are dissociated (CV $c \approx 2$), the average $d_{Ti5C-O2C}$ distance is 2.04 Å (see Figure 5), which is in quantitative agreement with the data obtained by surface X-ray diffraction (SXRD) for the ultrathin water film on the TiO_2(101) surface at room temperature.[38,39]

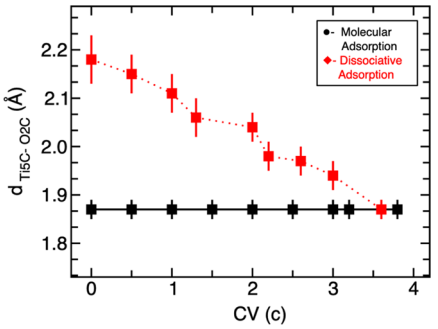

Figure 5. Mean values of Ti_{5C}−O_{2C} bond lengths ($d_{Ti5C-O2C}$, Å) with error bars versus CV (c) for dissociative (red line) and molecular (black line) adsorption metadynamics at θ = 1.

Overall, these results highlight that the stoichiometric TiO_2(101) surface has a non-zero probability to be partially hydroxylated at 300 K, with a quite favorable interface structure where 50% of the molecules underwent dissociation. The results are consistent with theoretical studies on this stochiometric anatase−water interface.[41] In addition, these results offer an explanation for experimental observations, although the anatase samples in the experiments are reduced rather than stoichiometric samples.[38−40]

CONCLUSIONS

In this work, we investigated the equilibrium between molecular and dissociative adsorption of water molecules on the TiO_2(101) surface by metadynamics simulations at the DFTB level of theory.

The formation of the first water molecular layer on Ti_{5C} is favored on the stoichiometric (101) facet with decreasing free energies for the second, third, and fourth H_2O adsorption processes. Nevertheless, at this low coverage, we predicted the presence of mixed H_2O/OH groups on the stoichiometric TiO_2(101) surface at room temperature, which is in qualitative agreement with recent experimental and theoretical works.[38−43] Strong Ti−O_W bonds and H_2O—OH interactions allow the dissociation barrier energy to be overcome, leading to an ultrathin partial dissociated water layer at the stoichiometric water−TiO_2(101) interface. These new insights into the structure and dynamics of the water−anatase interface call for a new perspective in future modeling of such interfaces, pointing out a possible role of partially hydroxylated (101) anatase stoichiometric surfaces.

AUTHOR INFORMATION

Corresponding Authors

Michele Pavone − *Department of Chemical Sciences, University of Naples Federico II, 80126 Napoli, Italy;* orcid.org/0000-0001-7549-631X; Email: mipavone@unina.it

https://doi.org/10.1021/acs.jpcc.2c03077
J. Phys. Chem. C 2022, 126, 15752−15758

Michele Parrinello − *Atomistic Simulations, Italian Institute of Technology, 16152 Genoa, Italy*; Email: michele.parrinello@phys.chem.ethz.ch

Authors

Francesca Fasulo − *Department of Chemical Sciences, University of Naples Federico II, 80126 Napoli, Italy*

GiovanniMaria Piccini − *Istituto Eulero, Università della Svizzera Italiana, 6900 Lugano, Switzerland*; orcid.org/0000-0002-3511-4281

Ana B. Muñoz-García − *Department of Physics "E. Pancini", University of Naples Federico II, 80126 Napoli, Italy*; orcid.org/0000-0002-9940-7358

Complete contact information is available at: https://pubs.acs.org/10.1021/acs.jpcc.2c03077

Author Contributions

The manuscript was written through contributions of all authors. All authors have given approval to the final version of the manuscript.

Notes

The authors declare no competing financial interest.

■ ACKNOWLEDGMENTS

This article was based upon a work by COST Action 18234, supported by COST (European Cooperation in Science and Technology). The authors also acknowledge COST Action 18234 for supporting a Short-Term Scientific Mission (STSM).

■ REFERENCES

(1) Tuller, H. L. Solar to Fuels Conversion Technologies: a Perspective. *Mater. Renew. Sustainable Energy* **2017**, *6*, No. 3.

(2) Harriman, A. Prospects for Conversion of Solar Energy into Chemical Fuels: the Concept of a Solar Fuels Industry. *Philos. Trans. R. Soc., A* **2013**, *371*, No. 20110415.

(3) Fujishima, A.; Honda, K. Electrochemical Photolysis of Water at a Semiconductor Electrode. *Nature* **1972**, *238*, 37−38.

(4) Walter, M. G.; Warren, E. L.; McKone, J. R.; Boettcher, S. W.; Mi, Q.; Santori, E. A.; Lewis, N. S. Solar Water Splitting Cells. *Chem. Rev.* **2010**, *110*, 6446−6473.

(5) Muñoz-García, A. B.; Benesperi, I.; Boschloo, G.; Concepcion, J. J.; Delcamp, J. H.; Gibson, E. A.; Meyer, G. J.; Pavone, M.; Pettersson, H.; Hagfeldt, A.; Freitag, M. Dye-Sensitized Solar Cells Strike Back. *Chem. Soc. Rev.* **2021**, *50*, 12450−12550.

(6) White, J. L.; Baruch, M. F.; Pander, J. E.; Hu, J.; Fortmeyer, I. C.; Park, J. E.; Zhang, T.; Liao, K.; Gu, J.; Yan, Y.; et al. Light-Driven Heterogeneous Reduction of Carbon Dioxide: Photocatalysts and Photoelectrodes. *Chem Rev.* **2015**, *115*, 12888−12935.

(7) Pavone, M.; Toroker, M. C. Toward Ambitious Multiscale Modeling of Nanocrystal Catalysts for Water Splitting. *ACS Energy Lett.* **2020**, *5*, 2042−2044.

(8) Kubacka, A.; Fernandez-Garcia, M.; Colon, G. Advanced Nanoarchitectures for Solar Photocatalytic Applications. *Chem. Rev.* **2012**, *112*, 1555−1614.

(9) Fan, J.; Liu, E. Z.; Tian, L.; Hu, X. Y.; He, Q.; Sun, T. Synergistic Effect of N and Ni^{2+} on Nanotitania in Photocatalytic Reduction of CO_2. *J. Environ. Eng.* **2011**, *137*, 171−176.

(10) Wang, C. J.; Thompson, R. L.; Baltrus, J.; Matranga, C. Visible Light Photoreduction of CO_2 Using CdSe/Pt/TiO_2 Heterostructured Catalysts. *J. Phys. Chem. Lett.* **2010**, *1*, 48−53.

(11) Ashley, M.; Magiera, C.; Ramidi, P.; Blackburn, G.; Scott, T. G.; Gupta, R.; Wilson, K.; Ghosh, A.; Biswas, A. Nanomaterials and Processes for Carbon Capture and Conversion into Useful by-Products for a Sustainable Energy Future. *Greenhouse Gases: Sci. Technol.* **2012**, *2*, 419−444.

(12) Dhakshinamoorthy, A.; Navalon, S.; Corma, A.; Garcia, H. Photocatalytic CO_2 Reduction by TiO_2 and Related Titanium Containing Solids. *Energy Environ. Sci.* **2012**, *5*, 9217−9233.

(13) De Angelis, F.; Di Valentin, C.; Fantacci, S.; Vittadini, A.; Selloni, A. Theoretical Studies on Anatase and Less Common TiO_2 Phases: Bulk, Surfaces, and Nanomaterials. *Chem. Rev.* **2014**, *114*, 9708−9753.

(14) Lettieri, S.; Gargiulo, V.; Alfè, M.; Amati, M.; Zeller, P.; Maraloiu, V. A.; Borbone, F.; Pavone, M.; Muñoz-García, A. B.; Maddalena, P. Simple Ethanol Refluxing Method for Production of Blue-Colored Titanium Dioxide with Oxygen Vacancies and Visible Light-Driven Photocatalytic Properties. *J. Phys. Chem. C* **2020**, *124*, 3564−3576.

(15) Lettieri, S.; Pavone, M.; Fioravanti, A.; Amato, L. S.; Maddalena, P. Charge Carrier Processes and Optical Properties in TiO_2 and TiO_2-Based Heterojunction Photocatalysts: A Review. *Materials* **2021**, *14*, 1645−1702.

(16) Linsebigler, A. L.; Lu, G.; Yates, J. T., Jr. Photocatalysis on TiO_2 Surfaces: Principles, Mechanisms, and Selected Results. *Chem. Rev.* **1995**, *95*, 735−758.

(17) Liu, L. J.; Zhao, C. Y.; Li, Y. Spontaneous Dissociation of CO_2 to CO on Defective Surface of Cu(I)/TiO_{2-x} Nanoparticles at Room Temperature. *J. Phys. Chem. C* **2012**, *116*, 7904−7912.

(18) Xi, G. C.; Ouyang, S. X.; Ye, J. H. General Synthesis of Hybrid TiO_2 Mesoporous "French Fries" Toward Improved Photocatalytic Conversion of CO_2 into Hydrocarbon Fuel: A Case of TiO_2/ZnO. *Chem.—Eur. J.* **2011**, *17*, 9057−9061.

(19) Low, J.; Cheng, B.; Yu, J. Surface Modification and Enhanced Photocatalytic CO_2 Reduction Performance of TiO_2: a Review. *Appl. Surf. Sci.* **2017**, *392*, 658−686.

(20) Anpo, M.; Hiromi, Y.; Yuichi, I.; Shaw, E. Photocatalytic Reduction of CO_2 with H_2O on Various Titanium Oxide Catalysts. *J. Electroanal. Chem.* **1995**, *396*, 21−26.

(21) Indrakanti, V. P.; Kubicki, J. D.; Schobert, H. H. Quantum Chemical Modeling of Ground States of CO_2 Chemisorbed on Anatase (001), (101), and (010) TiO_2 Surfaces. *Energy Fuels* **2008**, *22*, 2611−2618.

(22) Bourikas, K.; Kordulis, C.; Lycourghiotis, A. Titanium Dioxide (Anatase and Rutile): Surface Chemistry, Liquid−Solid Interface Chemistry, and Scientific Synthesis of Supported Catalysts. *Chem. Rev.* **2014**, *114*, 9754−9823.

(23) Barnard, A. S.; Zapol, P.; Curtiss, L. A. Modeling the Morphology and Phase Stability of TiO_2 Nanocrystals in Water. *J. Chem. Theory Comput.* **2005**, *1*, 107−116.

(24) Arrouvel, C.; Digne, M.; Breysse, M.; Toulhoat, H.; Raybaud, P. Effects of Morphology on Surface Hydroxyl Concentration: a DFT Comparison of Anatase−TiO_2 and γ-Alumina Catalytic Supports. *J. Catal.* **2004**, *222*, 152−166.

(25) Vittadini, A.; Selloni, A.; Rotzinger, F. P.; Gratzel, M. Structure and Energetics of Water Adsorbed at TiO_2 Anatase (101) and (001) Surfaces. *Phys. Rev. Lett.* **1998**, *81*, 2954−2957.

(26) Tilocca, A.; Selloni, A. Structure and Reactivity of Water Layers on Defect-Free and Defective Anatase TiO_2 (101) Surfaces. *J. Phys. Chem. B* **2004**, *108*, 4743−4751.

(27) Tilocca, A.; Selloni, A. Vertical and Lateral Order in Adsorbed Water Layers on Anatase TiO_2 (101). *Langmuir* **2004**, *20*, 8379−8384.

(28) Cheng, H.; Selloni, A. Hydroxide Ions at the Water/Anatase TiO_2 (101) Interface: Structure and Electronic States from first Principles Molecular Dynamics. *Langmuir* **2010**, *26*, 11518−11525.

(29) Selcuk, S.; Selloni, A. Facet-Dependent Trapping and Dynamics of Excess electrons at Anatase TiO_2 Surfaces and Aqueous Interfaces. *Nat. Mater.* **2016**, *15*, 1107−1112.

(30) Calegari Andrade, M. F.; Ko, H.; Car, R.; Selloni, A. Structure, Polarization, and Sum Frequency Generation Spectrum of Interfacial Water on Anatase TiO_2. *J. Phys. Chem. Lett.* **2018**, *9*, 6716−6721.

(31) Sumita, M.; Hu, C.; Tateyama, Y. Interface Water on TiO_2 Anatase (101) and (001) Surfaces: First-Principles Study with TiO_2

Slabs Dipped in Bulk Water. *J. Phys. Chem. C* **2010**, *114*, 18529−18537.
(32) Mattioli, G.; Filippone, F.; Caminiti, R.; Amore Bonapasta, A. Short Hydrogen Bonds at the Water/TiO_2 (Anatase) Interface. *J. Phys. Chem. C* **2008**, *112*, 13579−13586.
(33) Zhang, H.; Zhou, P.; Chen, Z.; Song, W.; Ji, H.; Ma, W.; Chen, C.; Zhao, J. Hydrogen-Bond Bridged Water Oxidation on {001} Surfaces of Anatase TiO_2. *J. Phys. Chem. C* **2017**, *121*, 2251−2257.
(34) Selli, D.; Fazio, G.; Seifert, G.; Di Valentin, C. Water Multilayers on TiO_2 (101) Anatase Surface: Assessment of a DFTB-Based Method. *J. Chem. Theory Comput.* **2017**, *13*, 3862−3873.
(35) Geng, Z.; Chen, X.; Yang, W.; Guo, W.; Xu, C.; Dai, D.; Yang, X. Highly Efficient Water Dissociation on Anatase TiO_2(101). *J. Phys. Chem. C* **2016**, *120*, 26807−26813.
(36) Herman, G. S.; Dohna'lek, Z.; Ruzycki, N.; Diebold, U. Experimental Investigation of the Interaction of Water and Methanol with Anatase-TiO_2(101). *J. Phys. Chem. B* **2003**, *107*, 2788−2795.
(37) Calegari Andrade, M. F.; Ko, H. Y.; Zhang, L.; Cara, R.; Selloni, A. Free Energy of Proton Transfer at the Water−TiO_2 Interface from Ab Initio Deep Potential Molecular Dynamics. *Chem. Sci.* **2020**, *11*, 2335−2341.
(38) Nadeem, I. M.; Treacy, J. P. W.; Selcuk, S.; Torrelles, X.; Hussain, H.; Wilson, A.; Grinter, D. C.; Cabailh, G.; Bikondoa, O.; Nicklin, C.; et al. Water Dissociates at the Aqueous Interface with Reduced Anatase TiO_2 (101). *J. Phys. Chem. Lett.* **2018**, *9*, 3131−3136.
(39) Jackman, M. J.; Thomas, A. G.; Muryn, C. Photoelectron Spectroscopy Study of Stoichiometric and Reduced Anatase TiO_2 (101) Surfaces: The Effect of Subsurface Defects on Water Adsorption at Near-Ambient Pressures. *J. Phys. Chem. C* **2015**, *119*, 13682−13690.
(40) Walle, L. E.; Borg, A.; Johansson, E. M. J.; Plogmaker, S.; Rensmo, H.; Uvdal, P.; Sandell, A. Mixed Dissociative and Molecular Water Adsorption on Anatase TiO_2(101). *J. Phys. Chem. C* **2011**, *115*, 9545−9550.
(41) Patrick, C. E.; Giustino, F. The Structure of a Water Monolayer on the Anatase TiO_2 (101) Surface. *Phys. Rev. Appl.* **2014**, *2*, No. 014001.
(42) Martinez-Casado, R.; Mallia, G.; Harrison, N. M.; Peŕez, R. First-Principles Study of the Water Adsorption on Anatase(101) as a Function of the Coverage. *J. Phys. Chem. C* **2018**, *122*, 20736−20744.
(43) Raju, M.; Kim, S.-Y.; van Duin, A. C. T.; Fichthorn, K. A. ReaxFF Reactive Force Field Study of the Dissociation of Water on Titania Surfaces. *J. Phys. Chem. C* **2013**, *117*, 10558−10572.
(44) Barducci, A.; Bonomi, M.; Parrinello, M. Metadynamics. *WIREs Comput. Mol. Sci.* **2011**, *1*, 826−843.
(45) Seifert, G. J. Tight-Binding Density Functional Theory: an Approximate Kohn−Sham DFT Scheme. *J. Phys. Chem. A* **2007**, *111*, 5609−5613.
(46) Frenzel, J.; Oliveira, A. F.; Jardillier, N.; Heine, T.; Seifert, G. F. *Semi-Relativistic, Self-Consistent Charge Slater-Koster Tables for Density-Functional Based Tight-Binding (DFTB) for Materials Science Simulations*; TU-Dresden: Dresden; 2004−2009.
(47) Luschtinetz, R.; Frenzel, J.; Milek, T.; Seifert, G. F. Adsorption of Phosphonic Acid at the TiO_2 Anatase (101) and Rutile (110) Surface. *J. Phys. Chem. C* **2009**, *113*, 5730−5740.
(48) Hutter, J.; Iannuzzi, M.; Schiffmann, F.; VandeVondele, J. CP2K: Atomistic Simulations of Condensed Matter Systems. *WIREs Comput. Mol. Sci.* **2014**, *4*, 15−25.
(49) Tribello, G. A.; Bonomi, M.; Branduardi, D.; Camilloni, C.; Bussi, G. PLUMED 2: New Feathers for an Old Bird. *Comput. Phys. Commun.* **2014**, *185*, 604−613.
(50) Bussi, G.; Donadio, D.; Parrinello, M. Canonical Sampling through Velocity Tescaling. *J. Chem. Phys.* **2007**, *126*, No. 014101.
(51) Sun, W.; Ceder, G. Efficient Creation and Convergence of Surface Slabs. *Surf. Sci.* **2013**, *617*, 53−59.
(52) Hamraoui, K.; Cristol, S.; Payen, E.; Paul, J. F. Computational Investigation of TiO_2-Supported Isolated Oxomolybdenum Species. *J. Phys. Chem. C* **2007**, *111*, 3963−3972.
(53) Perdew, J. P.; Burke, K.; Ernzerhof, M. Generalized Gradient Approximation Made Simple. *Phys. Rev. Lett.* **1996**, *77*, 3865−3868.
(54) O'Carroll, D.; English, N. J. A DFTB-Based Molecular Dynamics Investigation of an Explicitly Solvated Anatase Nanoparticle. *Appl. Sci.* **2022**, *12*, No. 780.
(55) Henkelman, G.; Uberuaga, B. P.; Jonsson, H. A Climbing Image Nudged Elastic Band Method for Finding Saddle Points and Minimum Energy Paths. *J. Chem. Phys.* **2000**, *113*, 9901−9904.
(56) Ferrighi, L.; Datteo, M.; Fazio, G.; Di Valentin, C. Catalysis under Cover: Enhanced Reactivity at the Interface between (Doped) Graphene and Anatase TiO_2. *J. Am. Chem. Soc.* **2016**, *138*, 7365−7376.
(57) Selli, D.; Fazio, G.; Di Valentin, C. Modelling Realistic TiO_2 Nanospheres: A Benchmark Study of SCC-DFTB Against Hybrid DFT. *J. Chem. Phys.* **2017**, *147*, No. 164701.
(58) Dahal, A.; Dohnalek, Z. Formation of Metastable Water Chains on Anatase TiO_2(101). *J. Phys. Chem. C* **2017**, *121*, 20413−20418.
(59) Zhao, Z.; Li, Z.; Zou, Z. Understanding the Interaction of Water with Anatase TiO_2 (101) Surface from Density Functional Theory Calculations. *Phys. Lett. A* **2011**, *375*, 2939−2945.
(60) Uehara, K.; Mizuno, N. Heterolytic Dissociation of Water Demonstrated by Crystal-to-Crystal Core Interconversion from (μ-Oxo)divanadium to Bis(μ-hydroxo)divanadium Substituted Polyoxometalates. *J. Am. Chem. Soc.* **2011**, *133*, 1622−1625.
(61) Ahdjoudj, J.; Minot, C. Adsorption of H_2O on Metal Oxides: a Periodic Ab-Initio Investigation. *Surf. Sci.* **1998**, *402*−*404*, 104−109.
(62) Wang, J. G.; Hammer, B. Theoretical Study of H_2O Dissociation and CO Oxidation on Pt_2Mo(111). *J. Catal.* **2006**, *243*, 192−198.
(63) Ishikawa, Y.; Diaz-Morales, R. R.; Perez, A.; Vilkas, M. J.; Cabrera, C. R. A Density-Functional Study of the Energetics of H_2O Dissociation on Bimetallic Pt/Ru Nanoclusters. *Chem. Phys. Lett.* **2005**, *411*, 404−410.

https://doi.org/10.1021/acs.jpcc.2c03077
J. Phys. Chem. C 2022, 126, 15752−15758